

Learning Q-function approximations for hybrid control problems

Sandeep Menta, Joseph Warrington, John Lygeros and Manfred Morari

Abstract—The main challenge in controlling hybrid systems arises from having to consider an exponential number of sequences of future modes to make good long-term decisions. Model predictive control (MPC) computes a control action through a finite-horizon optimisation problem. A key ingredient in this problem is a terminal cost, to account for the system’s evolution beyond the chosen horizon. A good terminal cost can reduce the horizon length required for good control action and is often tuned empirically by observing performance. We build on the idea of using N -step Q -functions ($Q^{(N)}$) in the MPC objective to avoid having to choose a terminal cost. We present a formulation incorporating the system dynamics and constraints to approximate the optimal $Q^{(N)}$ -function and algorithms to train the approximation parameters through an exploration of the state space. We test the control policy derived from the trained approximations on two benchmark problems through simulations and observe that our algorithms are able to learn good $Q^{(N)}$ -approximations for high dimensional hybrid systems based on a relatively small data-set. Finally, we compare our controller’s performance against that of Hybrid MPC in terms of computation time and closed-loop cost.

I. INTRODUCTION

Hybrid systems have been used to describe a range of real-world systems like solar energy plants [1], bipedal robots [2] and vehicle dynamics [3]. Hybrid systems allow one to use different dynamics at different parts of the state space at the price of having to include integer states or inputs complicating hybrid control problems. A popular control approach is hybrid Model Predictive Control (HMPC) that optimises over N -step trajectories with a terminal cost and/or constraints to account for the system evolution beyond the planning horizon. A well chosen terminal cost or constraint can reduce N , hence the computational effort required, but no general approach for making this choice exists. *Explicit MPC*, [4] methods reduce the online optimisation effort by computing the explicit feedback law defined over polyhedral partitions of states offline. For larger systems and longer horizon lengths the number of partitions can become prohibitive for online use. To reduce the computation Neural network (NN) based methods have emerged to approximate the explicit MPC laws by incorporating the model into their training procedures [5] or using specialised layers [6].

We follow the approach presented in [7] to use an N -step extension of the Q -function, $Q^{(N)}$, that takes as its arguments the first N states and actions. The optimal control policy

S.Menta, J.Warrington and J.Lygeros are with Automatic Control Lab, ETH Zürich, Physikstrasse 3, 8092 Zürich, Switzerland email: smenta@ethz.ch; joe.warrington@gmail.com; jlygeros@ethz.ch

M.Morari is with Elec. and Systems Engineering, Univ. of Pennsylvania, 220 S. 33rd St, Philadelphia, PA 19104, United States email: morari@seas.upenn.edu

can then be computed by minimising the optimal N -step Q -function ($Q^{(N)*}$), a process comparable to hybrid MPC. Our approach is to learn approximations of $Q^{(N)*}$ as a point-wise maximum of several lower bounding functions to $Q^{(N)*}$. The lower bounding functions are built by incorporating system dynamics and constraints. Our learning algorithm iteratively improves the approximation by adding tighter lower bounding functions at states chosen based on a metric of improvement. The advantage of our formulation is that it allows us to extract a control policy by solving a mixed-integer quadratic program (MIQP) of complexity comparable to HMPC instead of the computationally expensive *quadratically constrained* MIQCQP which results from the formulation proposed in [7].

We also test the necessity of utilising model information to achieve good control by using off-the-shelf NN training techniques and architectures, which do not use any model information, to learn the optimal control actions using the current state information. We compare the performance of our methods with HMPC and explicit controllers based on off-the-shelf NN training methods. Our simulation results on benchmark problems suggest that off-the-shelf NN training methods are not a good choice for hybrid control tasks and the controller derived from our approximations performs comparably to HMPC in terms of computational ease as well as the quality of the computed control actions.

The $Q^{(N)}$ -function and the control policy it generates are discussed in Section II. The algorithm used to approximate the $Q^{(N)*}$ is described in Section III and the simulation results on benchmark examples are presented in Section IV.

II. N-STEP Q -FUNCTION

A. Optimal V function

We consider the problem of optimal control for hybrid systems represented as time-invariant mixed logical dynamical (MLD) systems [8] without binary states or control inputs. Our starting point is an infinite horizon optimal control problem whose value function V^* is given by:

$$V^*(x) := \min_{\substack{\{x\}_0^\infty, \{u\}_0^\infty, \\ \{\delta\}_0^\infty, \{z\}_0^\infty}} \sum_{t=0}^{\infty} \frac{\gamma^t}{2} \begin{pmatrix} (x_t - x_g)^\top Q (x_t - x_g) + \\ (u_t - u_g)^\top R (u_t - u_g) \end{pmatrix} \quad (1a)$$

$$\text{s. t. } \begin{aligned} x_{t+1} &= Ax_t + B_1 u_t + B_2 \delta_t + B_3 z_t, \\ & \quad t = 0, 1, \dots, \end{aligned} \quad (1b)$$

$$E_2 \delta_t + E_3 z_t \leq E_4 x_t + E_1 u_t + E_5, \quad t = 0, 1, \dots, \quad (1c)$$

$$\begin{aligned}\delta_t &\in \{0, 1\}^{n_\delta}, \quad t = 0, 1, \dots, & (1d) \\ x_0 &= x, & (1e)\end{aligned}$$

where $x_t, x_g \in \mathbb{R}^n$ are the state and the goal state, $u_t, u_g \in \mathbb{R}^m$ are the input and the desired input, $z_t \in \mathbb{R}^{n_z}$ and δ_t are auxiliary continuous and binary variables required in the MLD framework. The shorthands $\{x\}_0^N$, are used to denote the sequences x_0, x_1, \dots, x_N , etc. We assume $Q \succ 0$ and $R \succ 0$. Constraints (1b)-(1e) ensure that the system evolves along feasible trajectories, including mode switches parameterized by δ_t . We assume the MLD system is “well-posed” [8], in the sense that x_t and u_t uniquely determine δ_t and z_t . The MLD constraints (1c) comprise the constraints that ensure the MLD system is “well-posed” and the state and input constraints which depend only on x_t and u_t , with n_c constraints per time step. The discount factor $\gamma \in (0, 1]$ is used here to include a wider class of problems, for example, problems with periodic solutions.

B. Hybrid MPC

HMPC involves computing the optimal control actions by minimising an approximation of $V^*(x)$. The objective of HMPC uses the first N -terms from (1) and approximates the rest of the summation via a terminal cost $V(x_N)$. This formulation using the truncated objective can be found in [9, §17.4]. The ideal terminal cost would be the optimal cost function $V^*(x_N)$ itself but $V^*(x)$ is in general impossible to compute. To reduce the effect of truncating the infinite horizon problem and using a sub-optimal terminal cost the HMPC controller is used in a receding horizon fashion.

C. Optimal N -step \mathcal{Q} -function

The notion of a N -step \mathcal{Q} -function introduced in [7] takes the initial state x_0 and a N -step feasible sequence of inputs and auxiliary variables $(\{u, \delta, z\}_0^N)$ as its parameters. Though redundant due to well-posedness, without loss of generality one can also include $\{x\}_1^N$ as arguments. The optimal N -step \mathcal{Q} -function ($\mathcal{Q}^{(N)*}$) associated with this parametrization of the $\mathcal{Q}^{(N)}$ -function can be obtained in the same way the optimal value function is computed:

$$\begin{aligned}\mathcal{Q}^{(N)*}(\{x\}_0^{N-1}, \{u\}_0^{N-1}, \{\delta\}_0^{N-1}, \{z\}_0^{N-1}) := \\ \min_{\substack{\{x\}_1^N, \{u\}_1^N, \\ \{\delta\}_1^N, \{z\}_1^N}} \sum_{t=0}^{\infty} \frac{\gamma^t}{2} \left((x_t - x_g)^\top Q (x_t - x_g) + \right. \\ \left. (u_t - u_g)^\top R (u_t - u_g) \right) & (2) \\ \text{s.t. (1b)-(1e)}\end{aligned}$$

which implies that

$$\begin{aligned}\mathcal{Q}^{(N)*}(\{x\}_0^{N-1}, \{u\}_0^{N-1}, \{\delta\}_0^{N-1}, \{z\}_0^{N-1}) = \\ \sum_{t=0}^{N-1} \frac{\gamma^t}{2} (x_t - x_g)^\top Q (x_t - x_g) + \\ \sum_{t=0}^{N-1} \frac{\gamma^t}{2} (u_t - u_g)^\top R (u_t - u_g) + \gamma^N V^*(x_N), & (3)\end{aligned}$$

where $\{x\}_0^N, \{u\}_0^N, \{\delta\}_0^N, \{z\}_0^N$ satisfy the constraints (1b)-(1e). To simplify notation we introduce $s = (x, u, \delta, z) \in \mathbb{R}^n \times \mathbb{R}^m \times \{0, 1\}^{n_\delta} \times \mathbb{R}^{n_z}$. The state x along with the inputs and auxiliary variables compatible with it can then be

described by the set $\mathcal{S}(x) := \{s = (x, u, \delta, z) \in \mathbb{R}^n \times \mathbb{R}^m \times \{0, 1\}^{n_\delta} \times \mathbb{R}^{n_z} : E_2\delta + E_3z \leq E_4x + E_1u + E_5\}$ and the set of N -step feasible trajectories from the initial state x ,

$$\mathcal{S}^{(N)}(x) := \left\{ \begin{aligned} \{s\}_0^{N-1} &= \{x, u, \delta, z\}_0^{N-1} : x_0 = x, \\ x_{k+1} &= Ax_k + B_1u_k + B_2\delta_k + B_3z_k, \\ s_k &\in \mathcal{S}(x_k) \text{ for } k = 0, \dots, N-1 \end{aligned} \right\} & (4)$$

Following [7], a greedy control policy can be extracted from a $\mathcal{Q}^{(N)}$ -function as follows:

$$\pi(x; \mathcal{Q}^{(N)}) \in \left[\arg \min_{\{s\}_0^{N-1} \in \mathcal{S}^{(N)}(x)} \mathcal{Q}^{(N)}(\{s\}_0^{N-1}) \right]_{u_0} & (5)$$

The notation $[\cdot \dots]_{u_0}$ shows that the control input u_0 is taken from the optimal s_0 , assuming an optimum is attained. We can conclude from (2) that $\pi(x; \mathcal{Q}^{(N)*})$ is an optimal policy that gives the optimal infinite-horizon “closed-loop” cost $V^*(x)$ when applied recursively.

III. NOVEL APPROXIMATE $\mathcal{Q}^{(N)*}$ -FORMULATION

The ease of extracting the control policy in (5) depends heavily on the structure of the $\mathcal{Q}^{(N)}$ -function. Here we construct an approximation of $\mathcal{Q}^{(N)*}$ as a point-wise maximum of several lower bounding functions referred to as “cuts”. Our formulation of the lower bounding functions builds on [7] and addresses some key difficulties arising there.

A. Bellman operator for N -step $\mathcal{Q}^{(N)}$ -functions

The Bellman operator $\mathcal{T}_{\mathcal{Q}}^{(N)}$ for a generic function $\mathcal{Q}^{(N)}$ for a feasible trajectory $\{s\}_0^{N-1}$ starting at x_0 is defined as:

$$\begin{aligned}\mathcal{T}_{\mathcal{Q}}^{(N)} \mathcal{Q}^{(N)}(\{s\}_0^{N-1}) &= \frac{1}{2} (x_0 - x_g)^\top Q (x_0 - x_g) + \\ &\frac{1}{2} (u_0 - u_g)^\top R (u_0 - u_g) + \inf_{s_N \in \mathcal{S}(x_N)} \gamma \mathcal{Q}^{(N)}(\{s\}_1^N). & (6)\end{aligned}$$

From (2) and (6), for all $x_0 \in \mathbb{R}^n$, $\{s\}_0^{N-1} \in \mathcal{S}^{(N)}(x_0)$ we have $\mathcal{Q}^{(N)*}$ is a fixed point of $\mathcal{T}_{\mathcal{Q}}^{(N)}$, that is $\mathcal{T}_{\mathcal{Q}}^{(N)} \mathcal{Q}^{(N)*}(\{s\}_0^{N-1}) = \mathcal{Q}^{(N)*}(\{s\}_0^{N-1})$. Moreover, $\mathcal{T}_{\mathcal{Q}}^{(N)}$ is monotonic, that is, if $\mathcal{Q}_a^{(N)}(\{s\}_0^{N-1}) \leq \mathcal{Q}_b^{(N)}(\{s\}_0^{N-1})$ for all $x_0 \in \mathbb{R}^n$, $\{s\}_0^{N-1} \in \mathcal{S}^{(N)}(x_0)$, then

$$\begin{aligned}\mathcal{T}_{\mathcal{Q}}^{(N)} \mathcal{Q}_a^{(N)}(\{s\}_0^{N-1}) &\leq \mathcal{T}_{\mathcal{Q}}^{(N)} \mathcal{Q}_b^{(N)}(\{s\}_0^{N-1}), \\ \forall x_0 \in \mathbb{R}^n, \{s\}_0^{N-1} &\in \mathcal{S}^{(N)}(x_0).\end{aligned}$$

B. Reformulated Benders’ cuts

The approximation of $\mathcal{Q}^{(N)*}$ constructed as a point-wise maximum of $I + 1$ cuts q_0, q_1, \dots, q_I is given by:

$$\mathcal{Q}_I^{(N)}(\{s\}_0^{N-1}) := \max_{i=0, \dots, I} \{q_i(\{s\}_0^{N-1})\}, & (7)$$

where each of the cuts satisfies,

$$\begin{aligned}q_i(\{s\}_0^{N-1}) &\leq \mathcal{Q}^{(N)*}(\{s\}_0^{N-1}), \\ \forall x_0 \in \mathbb{R}^n, \{s\}_0^{N-1} &\in \mathcal{S}^{(N)}(x_0) & (8)\end{aligned}$$

This results in an approximation which lower bounds $\mathcal{Q}^{(N)*}$ everywhere. Following [7], [10] we choose the cuts to be linearly separable in their arguments:

$$q_i(\{s\}_0^{N-1}) = \sum_{j=0}^{N-1} q_i^{x_j}(x_j) + \sum_{j=0}^{N-1} q_i^{u_j}(u_j) + \sum_{j=0}^{N-1} q_i^{\delta_j}(\delta_j) + \sum_{j=0}^{N-1} q_i^{z_j}(z_j) + c_i, \quad (9)$$

where $\{s\}_0^{N-1} \in \mathcal{S}^{(N)}(x_0)$ and each of the $q_i^{(\cdot)}(\cdot)$ terms are linear and convex quadratic functions, and c_i is a constant term. Cut q_0 is the starting point for building the approximation:

$$q_0(\{s\}_0^{N-1}) = \sum_{t=0}^{N-1} \frac{\gamma^t}{2} (x_t - x_g)^\top Q (x_t - x_g) + \sum_{t=0}^{N-1} \frac{\gamma^t}{2} (u_t - u_g)^\top R (u_t - u_g). \quad (10)$$

From (3), q_0 is clearly a lower bounding function to $\mathcal{Q}^{(N)*}$, as $V^*(x_N) \geq 0$. The first step in this process is to apply the Bellman operator to the existing approximation $\mathcal{Q}_I^{(N)}$ at $\{s\}_0^{N-1} \in \mathcal{S}^{(N)}(x_0)$:

$$\mathcal{T}_{\mathcal{Q}}^{(N)} \mathcal{Q}_I^{(N)}(\{s\}_0^{N-1}) = \inf_{x_N, s_N, \alpha} \left(\frac{1}{2} (x_0 - x_g)^\top Q (x_0 - x_g) + \frac{1}{2} (u_0 - u_g)^\top R (u_0 - u_g) + \gamma \alpha \right) \quad (11a)$$

$$\text{s. t. } x_N = Ax_{N-1} + B_1 u_{N-1} + B_2 \delta_{N-1} + B_3 z_{N-1} \quad (11b)$$

$$E_2 \delta_N + E_3 z_N \leq E_1 u_N + E_4 x_N + E_5, \quad (11c)$$

$$q_i(\{s\}_1^N) \leq \alpha, \quad i = 0, \dots, I \quad (11d)$$

where the value of $\mathcal{Q}_I^{(N)}(\{s\}_1^N)$ is modelled by the epigraph variable α . The form of the terms in the cuts (9) comes from the objective function of the dual of (11). We derive the dual by assigning multipliers $\nu \in \mathbb{R}^n$ to (11b), $\mu \in \mathbb{R}^{n_c}$ to (11c) and $\lambda \in \mathbb{R}^{I+1}$ to (11d). The dual is then written as the operator $\mathcal{D}^{(N)}$ acting on $\mathcal{Q}_I^{(N)}$:

$$\mathcal{D}^{(N)} \mathcal{Q}_I^{(N)}(\{s\}_0^{N-1}) := \sup_{\nu, \mu, \lambda} \left\{ \begin{array}{l} \frac{1}{2} (x_0 - x_g)^\top Q (x_0 - x_g) + \sum_{i=1}^I \lambda_i c_i + \\ \frac{1}{2} (u_0 - u_g)^\top R (u_0 - u_g) - \mu^\top E_5 + \xi(\nu, \mu, \lambda) + \\ \nu^\top (Ax_{N-1} + B_1 u_{N-1} + B_2 \delta_{N-1} + B_3 z_{N-1}) + \\ \sum_{i=0}^I \lambda_i \sum_{t=1}^{N-1} \left(q_i^{x_{t-1}}(x_t) + q_i^{u_{t-1}}(u_t) + \right. \\ \left. q_i^{\delta_{t-1}}(\delta_t) + q_i^{z_{t-1}}(z_t) \right) \end{array} \right\} \quad (12a)$$

$$\text{s. t. } \mu \geq 0, \quad \lambda \geq 0, \quad \mathbf{1}^\top \lambda = \gamma, \quad (12b)$$

where,

$$\xi(\nu, \mu, \lambda) := \inf_{s^N} \left\{ \begin{array}{l} \mu^\top (E_2 \delta_N + E_3 z_N - E_1 u_N - E_4 x_N) + \\ \sum_{i=0}^I \lambda_i \left(q_i^{x_{N-1}}(x_N) + q_i^{u_{N-1}}(u_N) + \right. \\ \left. q_i^{\delta_{N-1}}(\delta_N) + q_i^{z_{N-1}}(z_N) \right) - \nu^\top x_N \end{array} \right\}.$$

The form of the new cut q_{I+1} constructed using the optimal dual multipliers $(\nu^*, \mu^*, \lambda^*)$ is shown in Lemma 3.1.

Lemma 3.1: The function

$$q_{I+1}(\{s\}_0^{N-1}) := \sum_{t=0}^{N-1} q_{I+1}^{x_t}(x_t) + \sum_{t=0}^{N-1} q_{I+1}^{u_t}(u_t) + \sum_{t=0}^{N-1} q_{I+1}^{\delta_t}(\delta_t) + \sum_{t=0}^{N-1} q_{I+1}^{z_t}(z_t) + c_{I+1}, \quad (13)$$

satisfies the global lower bounding property

Algorithm 1 Modified Benders algorithm for MLD systems

- 1: **Inputs:** System model; training points $\mathcal{X}_{\text{Alg}} := \{x^1, \dots, x^M\}$, I_{max} , η_{min} and $q_0(\{s\}_0^{N-1})$
 - 2: Set $I = 0$, $\eta^* = \infty$
 - 3: **while** $I \leq I_{\text{max}}$ and $\eta^* \geq \eta_{\text{min}}$ **do**
 - 4: $\mathcal{Q}_I^{(N)}(\cdot) \leftarrow \max_{i=0, \dots, I} q_i(\cdot)$
 - 5: **for each** $x \in \mathcal{X}_{\text{Alg}}$ **do**
 - 6: $\{s\}_0^{N-1} \leftarrow \arg \min_{\{s\}_0^{N-1} \in \mathcal{S}^{(N)}(x)} \left\{ \mathcal{Q}_I^{(N)}(\{s\}_0^{N-1}) \right\}$
 - 7: $\eta(\{s\}_0^{N-1}; \mathcal{Q}_I^{(N)}) \leftarrow \tilde{\beta}(\{s\}_0^{N-1}; \mathcal{Q}_I^{(N)})$
 - 8: **end for**
 - 9: $x^*, \{s^*\}_0^{N-1} \leftarrow \arg \max_{\substack{x \in \mathcal{X}_{\text{Alg}}, \\ \{s\}_0^{N-1} \in \mathcal{S}^{(N)}(x)}} \left\{ \eta(\{s\}_0^{N-1}; \mathcal{Q}_I^{(N)}) \right\}$
 - 10: **if** $\eta^* = \eta(x^*, \{s^*\}_0^{N-1}; \mathcal{Q}_I^{(N)}) \geq \eta_{\text{min}}$ **then**
 - 11: Add $q_{I+1}(\cdot)$ parameterized by the $(\nu^*, \mu^*, \lambda^*)$ optimal for problem (12) with the parameter $(x^*, \{s^*\}_0^{N-1})$ to the set of $q_i(\cdot)$ functions
 - 12: **end if**
 - 13: $I \leftarrow I + 1$
 - 14: **end while**
 - 15: **Output:** $\mathcal{Q}_I^{(N)}(\cdot) = \max_{i=0, \dots, I} q_i(\cdot)$
-

$$q_{I+1}(\{s\}_0^{N-1}) \leq \mathcal{Q}^{(N)*}(\{s\}_0^{N-1}), \quad \forall x_0 \in \mathbb{R}^n, \{s\}_0^{N-1} \in \mathcal{S}^{(N)}(x_0)$$

where,

$$\begin{aligned} q_{I+1}^{x_t}(x_t) &= \frac{\gamma^t}{2} (x_t - x_g)^\top Q (x_t - x_g), & q_{I+1}^{\delta_t}(\delta_t) &= 0, \\ q_{I+1}^{u_t}(u_t) &= \frac{\gamma^t}{2} (u_t - u_g)^\top R (u_t - u_g), & q_{I+1}^{z_t}(z_t) &= 0, \\ q_{I+1}^{x_{N-1}}(x_{N-1}) &= \gamma q_{I+1}^{x_{N-2}}(x_{N-1}) + \nu^{*\top} A x_{N-1} \\ q_{I+1}^{u_{N-1}}(u_{N-1}) &= \gamma q_{I+1}^{u_{N-2}}(u_{N-1}) + \nu^{*\top} B_1 u_{N-1}, \\ q_{I+1}^{\delta_{N-1}}(\delta_{N-1}) &= \nu^{*\top} B_2 \delta_{N-1}, & q_{I+1}^{z_{N-1}}(z_{N-1}) &= \nu^{*\top} B_3 z_{N-1}, \\ c_{I+1} &= \sum_{i=1}^I \lambda_i^* c_i - \mu^{*\top} E_5 + \xi(\nu^*, \mu^*, \lambda^*), \end{aligned}$$

for $t = 0, \dots, N-2$ and the triplet $(\nu^*, \mu^*, \lambda^*)$ solves problem (12) for the parameter $\{s\}_0^{N-1} \in \mathcal{S}^{(N)}(\hat{x}_0)$.

The proof is a simple adaptation of the proof of Lemma III.1 in [7]. Lemmas III.2-4 of [10] carry over to the present setting but are omitted in the interest of space. We highlight that the addition of the new cut q_{I+1} at the parameter $\{s\}_0^{N-1} \in \mathcal{S}^{(N)}(x_0)$ leads to an improvement of $\mathcal{D}^{(N)} \mathcal{Q}_I^{(N)}(\{s\}_0^{N-1}) - \mathcal{Q}_I^{(N)}(\{s\}_0^{N-1})$ in the approximation at $\{s\}_0^{N-1}$. Lemma 3.1 shows that each cut is the sum of N stage costs along with a penalty on the N^{th} state and a constant. Thus, the generated approximation is the standard MPC objective with a terminal cost approximation that naturally incorporates the system dynamics and constraints.

C. Training algorithm

The approximation of $\mathcal{Q}^{(N)*}$ is learnt iteratively by searching over a given set of data points \mathcal{X}_{Alg} . At each point in \mathcal{X}_{Alg} the N -step greedy policy is evaluated using the current approximation $\mathcal{Q}_I^{(N)}$, and an improvement metric is evaluated and stored. A new cut is then added at the point

which promises the highest improvement, as described in Algorithm 1. We propose the metric $\tilde{\beta}$ building on β [7] :

$$\beta(x; \mathcal{Q}_I^{(N)}) := \mathcal{D}^{(N)} \mathcal{Q}_I^{(N)}(\{s\}_0^{N-1}) - \mathcal{Q}_I^{(N)}(\{s\}_0^{N-1}), \quad (14)$$

$$\tilde{\beta}(x; \mathcal{Q}_I^{(N)}) := \beta(x; \mathcal{Q}_I^{(N)}) / \mathcal{Q}_I^{(N)}(\{s\}_0^{N-1}). \quad (15)$$

$\tilde{\beta}$ is a normalised metric which measures the improvement along the trajectory $\{s\}_0^{N-1}$ relative to the value of the $\mathcal{Q}_I^{(N)}$ there resulting from the addition of a cut at x . In our numerical investigation we observe that using β leads to more cuts at points “far” from the goal states, leading to a richer function approximation there. Using $\tilde{\beta}$, on the other hand, adds cuts closer to the goal states, at points that lead to the highest improvement relative to the value of the $\mathcal{Q}^{(N)}$ -function.

D. Advantages of the new formulation

An efficient implementation that computes the policy (5) using an approximation of form (7) uses as its objective function the common terms from all the cuts that build the approximation $\mathcal{Q}_I^{(N)}$ and an epigraph variable α lower bounded by the terms remaining in the cuts. The formulation of the cuts presented in [7, Lemma 3.1] leads to a MIQCQP due to the extra quadratic terms present in q_0 , whereas, our formulation (13) gives rise to the following simpler MIQP,

$$\begin{aligned} \min_{\{s\}_0^{N-1}} & \sum_{t=0}^{N-1} \left(\frac{\gamma^t}{2} (x_t - x_g)^\top Q (x_t - x_g) + \frac{\gamma^t}{2} (u_t - u_g)^\top R (u_t - u_g) \right) + \alpha \\ \text{s.t.} & \{s\}_0^{N-1} \in \mathcal{S}^{(N)}(x_0) \\ & \nu_i^* (Ax_{N-1} + B_1 u_{N-1} + B_2 \delta_{N-1} + B_3 z_{N-1}) + c_i \leq \alpha, \\ & i = 1, \dots, I, \end{aligned}$$

where the ν_i^* is the optimal dual multiplier used in q_i . The removal of the quadratic constraints arising from q_0 leads to a significant reduction of the policy computation times.

The cuts we generate add linear terms in addition to the quadratic terms present in cut q_0 , removing the advantage q_0 enjoyed in [7] where the extra quadratic terms dominated the added linear terms, especially, closer to the goal states. In combination with the proposed metric $\tilde{\beta}$, compared to the formulation in [7], our formulation is able to add more cuts that build the $\mathcal{Q}_I^{(N)}$ closer to the goal states giving a richer approximation there, this leads to better closed-loop performance as the trajectories from any initial condition definitely traverse this region to reach x_g .

IV. NUMERICAL EXAMPLES

We test the performance of the resulting controller on a traction control problem [3] and a boiler-turbine system [11].

A. Traction control

A traction controller is used to improve the stability and steerability of a vehicle under slippery conditions. The controller aims to control the *slip* between the tires and the road to maximise the frictional torque. The frictional torque depends on slip through a non-linear relation, which is approximated as a piecewise affine function with 2 regions, leading to hybrid vehicle dynamics with 2 modes [3].

1) *System dynamics*: The dynamics of the vehicle [3, (7)] are modelled as an MLD system with the following matrices:

$$A = \begin{bmatrix} 1 & 0 & 0 \\ 4.8792 \cdot 10^{-2} & 1.0005 & -2.1835 \cdot 10^{-2} \\ -1.5695 \cdot 10^{-7} & -6.4359 \cdot 10^{-6} & 1.0003 \end{bmatrix}, \quad (16)$$

$$B_1 = \begin{bmatrix} 1 & 0 \\ 4.8792 \cdot 10^{-2} & -6.5287 \\ -1.5695 \cdot 10^{-7} & 8.9695 \cdot 10^{-2} \end{bmatrix}, \quad (17)$$

$$B_2 = \begin{bmatrix} 0 & 0 \\ 0.10943 & 0.81687 \\ -1.5034 \cdot 10^{-3} & -1.1223 \cdot 10^{-2} \end{bmatrix}, \quad B_3 = \begin{bmatrix} 0 & 0 \\ 1 & 0 \\ 0 & 1 \end{bmatrix}. \quad (18)$$

The states are $x = [\tau_c^- \ \omega_e \ v_v]^\top$, where τ_c^- is the combustion torque applied at the previous time step, ω_e is the engine speed, v_v is the vehicle velocity. The inputs are $u = [\Delta\tau_c \ \mu_s]^\top$, where $\Delta\tau_c$ is the change in the combustion torque and μ_s is the coefficient of friction between the tire and the road, an uncontrolled input that is estimated and given to the controller [3, Sec. VI.C]. The auxiliary binary variables $\delta = [\delta_1 \ \delta_2]^\top$, describe the modes of operation of the vehicle dynamics and the auxiliary continuous variables $z = [z_1 \ z_2]^\top$ capture the mode dependent dynamics of the system. Slip ($\Delta\omega$) at a given time step is computed as:

$$\Delta\omega = \frac{v_v}{r_t} - \frac{\omega_e}{g_r} = \underbrace{\begin{bmatrix} 0 & -\frac{1}{g_r} & \frac{1}{r_t} \end{bmatrix}}_{S_x} x = S_x x,$$

where r_t is the tire radius and g_r is the driveline gear ratio. The following constraints apply to the dynamics:

$$-20 \leq \tau_c \leq 176, \quad -40 \leq \Delta\tau_c \leq 40, \quad \Delta\omega \geq 0. \quad (19)$$

The constraints ensuring well-posedness and (19) form the MLD constraints for this system where $n_c = 25$. The MLD constraint matrices are given in the Appendix.

2) *Stage cost function*: It is observed that the frictional torque is the highest at the line separating the 2 regions of operation. We make the assumption that μ_s is fixed, resulting in a piecewise affine relation between slip and frictional torque. Hence, the control problem is to steer the system to the switching boundary, as that maximises the frictional torque, with a penalty on changing combustion torque. We choose the following quadratic stage cost function:

$$\begin{aligned} \ell(x, u) &= \frac{1}{2} \cdot 50 \cdot (\Delta\omega - \Delta\omega_g)^2 + \frac{1}{2} \cdot 0.1 \cdot (\Delta\tau_c)^2 \\ &= \frac{1}{2} (x - x_g)^\top Q (x - x_g) + \frac{1}{2} (u - u_g)^\top R (u - u_g) \end{aligned} \quad (20)$$

$$Q = \begin{bmatrix} 0 & 0 & 0 \\ 0 & 0.259 & -12.08 \\ 0 & -12.08 & 563.04 \end{bmatrix} \quad R = \begin{bmatrix} 0.1 & 0 \\ 0 & 0 \end{bmatrix}$$

Since we have $Q \succeq 0$ and $R \succeq 0$, we shift their eigenvalues by a small $\epsilon = 10^{-9}$ to make them positive definite, this shift has a negligible impact on performance. We choose $\mu_s = 0.1934$ which results in $\Delta\omega_g = 2$ and any x_g that satisfies $\Delta\omega_g = S_x x_g$ and $u_g = [0 \ \mu_s]^\top$.

TABLE I
COMPARISON OF CLOSED-LOOP COSTS AGAINST HMPC FOR THE TRACTION CONTROL EXAMPLE

Baseline	π_1 : HMPC $N = 30$			π_1 : HMPC $N = 15$		
	% of points where π_1 is better than the baseline	Mean better performance (%) at points where π_1 is better	Mean worse performance (%) at points where π_1 is worse	% of points where π_1 is better than the baseline	Mean better performance (%) at points where π_1 is better	Mean worse performance (%) at points where π_1 is worse
$\pi(x; \underline{Q}_{22}^{(15)})$	48.7	0.12	0.08	25.7	0.11	1.53
HMPC $N = 15$	90.2	1.26	0.13	-	-	-

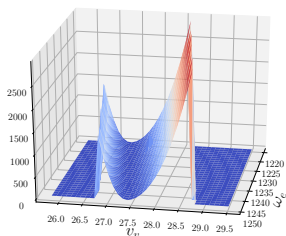


Fig. 1. Plot of $V^*(x)$ for the traction control problem

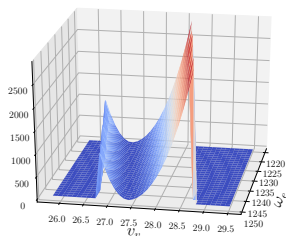


Fig. 2. Plot of $\underline{Q}_{22}^{(15)}(x)$ for the traction control problem

3) $\underline{Q}^{(N)}$ -function approximation: The $\underline{Q}^{(N)}$ -function is learnt with $N = 15$, over \mathcal{X}_{Alg} with 22 data points spread over the slip range $[0, 0.15]$, $I_{\text{max}} = 100$ and $\eta_{\text{min}} = 10^{-5}$. The generated approximation $\underline{Q}_{22}^{(15)}$ has $I = 22$.

As the system dimension is small, we approximate $V^*(x)$ by using HMPC with a long horizon length of 30 for the points in the slip range $[0, 0.6.5]$. For the purposes of visualisation of the trained $\underline{Q}^{(N)}$ -functions we define

$$\underline{Q}^{(N)}(x) = \inf_{\{s\}_0^{N-1} \in \mathcal{S}^{(N)}(x)} \underline{Q}^{(N)}(\{s\}_0^{N-1}).$$

Evaluating $\underline{Q}^{(N)}$ gives us an idea of the approximation quality as $\underline{Q}^{(N)*}(x) = V^*(x)$. The plots of V^* and the $\underline{Q}_{22}^{(15)}$ are shown in Figs. 1 and 2, for the slip range $[0, 0.6.5]$. Figs. 1 and 2 suggest that the $\underline{Q}^{(N)}$ -function approximates the optimal value function very well.

4) Simulations using $\underline{Q}_I^{(N)}$: We compare the closed-loop costs of applying the control policy (5), derived from $\underline{Q}_{22}^{(15)}$, against those of HMPC, with the LQR terminal cost derived using A and B_1 matrices, from 470 initial conditions spread across the slip range $[0, 0.6.5]$.

Table I presents a detailed comparison of the closed-loop costs induced by the different controllers from the 470 initial conditions. The closed-loop costs of our method and HMPC $N = 15$ are on an average 0.02% and 1.1% worse than the values of $V^*(x)$ respectively, which shows that our control policy is effectively identical to the optimal control policy. Our controller $\pi(x; \underline{Q}_{22}^{(15)})$ clearly performs better than HMPC of the same horizon length, as seen from the entries of Table I. The points where HMPC $N = 15$ and our controller outperform HMPC $N = 30$, it is observed that they do so by very small values due to numerical effects. The $\Delta\omega$ trajectories resulting from $\pi(x; \underline{Q}_{22}^{(15)})$ are shown in

Fig. 3. The average time taken to compute the policy across the 470 initial conditions is 0.132s for HMPC $N = 15$, 0.141s for $\pi(x; \underline{Q}_{22}^{(15)})$ and 0.394s for HMPC $N = 30$. For the sake of comparison, solving the MIQCQP to compute the controller of [7] for this system using an approximation with the same N and I would require in excess of 0.25s. On computing $\underline{Q}_{22}^{(6)}$ at 2327 points in the slip range $[0, 0.6.5]$, it is seen that the q_0 is used at only 34 points, whereas, an approximation trained with the same parameters and metric using the formulation in [7] uses q_0 at 1357 of these points.

We also tested the effect of using $\pi(x; \underline{Q}_{22}^{(15)})$ on the system when μ_s was different than the value used in training. We observed that when the difference between $\Delta\omega_g$ and *slip at the switching boundary* is not large our controller drives the slip of the system to the one closer to the initial state. Since μ_s can change dramatically, one can train \underline{Q} -functions for various values of μ_s and control the vehicle using the \underline{Q} -function trained with the μ_s closest to the estimated one.

To compare against model-free techniques we train a Fully Connected Neural Network with a Sigmoid activation at the last layer and ReLU activations elsewhere using data from HMPC $N = 30$. The network predicts τ_c using $\omega_e, v_v, \Delta\omega, \tau_c$ and the region number. We used BOHB [12] to find a good architecture searching over models with 4-7 layers with 8-64 neurons each and over the range $[10^{-1}, 10^{-4}]$ for the learning rate. The models were trained and tested using 75927 and 31637 data points respectively. The best model had 2,776 parameters and gave a mean test error of 0.186% with a variance of 0.223%. The resulting controller, resulted in large oscillations at the switching boundary due to the high sensitivity of the dynamics to τ_c there. Fig. 4 shows the trajectories resulting from the use of the NN controller from the same initial states as in Fig. 3. This suggests that

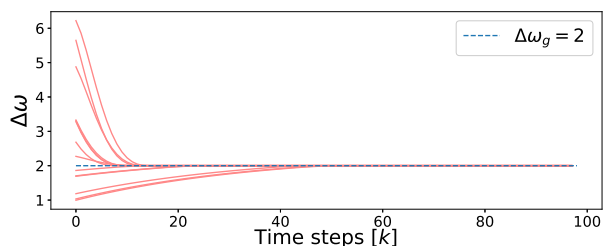


Fig. 3. Slip trajectories generated by $\pi(x; \underline{Q}_{22}^{(15)})$

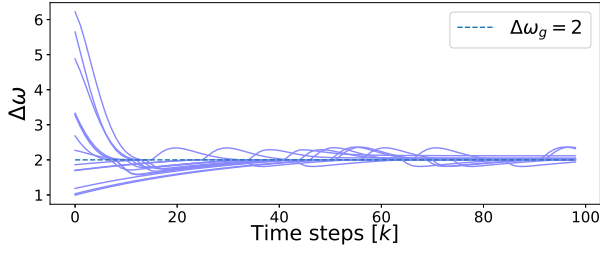


Fig. 4. Slip trajectories generated by the best NN model

off-the shelf neural network techniques might not be the best choice for hybrid problems due to the switching dynamics compared to other methods that approximate explicit MPC using model information [5], [6].

B. Boiler-turbine system

A boiler-turbine system converts chemical energy from burning fuels to electrical energy via a steam boiler and a turbine. The boiler-turbine system has been widely studied with a variety of control techniques. This system has several nominal operating points [11] and we want to steer the system to the “normal” nominal operating point starting from some other state.

1) *System dynamics*: The non-linear dynamics of the system [11, eqn. (3), (5)] are given by

$$\frac{dp}{dt} = -0.0018u_2p^{9/8} + 0.9u_1 - 0.15u_3, \quad (21a)$$

$$\frac{dp_0}{dt} = (0.073u_2 - 0.016)p^{9/8} - 0.1p_0, \quad (21b)$$

$$\frac{dp_f}{dt} = \frac{141u_3 - (1.1u_2 - 0.19)p}{85}, \quad (21c)$$

$$X_w = 0.05 \left(0.1307p_f + 100\alpha_{cs} + \frac{q_e}{9} - 67.975 \right), \quad (21d)$$

$$\alpha_{cs} = \frac{(1 - 0.001538p_f)(0.8p - 25.6)}{p_f(1.0394 - 0.0012304p)}, \quad (21e)$$

$$q_e = (0.854u_2 - 0.147)p + 45.59u_1 - 2.514u_3 - 2.096, \quad (21f)$$

where p is the drum pressure (kg/cm^2), p_0 the power output (MW) and p_f the fluid density (kg/cm^3). The inputs u_1 , u_2 and u_3 respectively control fuel flow valve position, steam control valve position and feed-water flow valve position and lie in the interval $[0, 1]$. X_w , q_e and α_{cs} denote the drum water level (m), the evaporation rate (kg/s) and the steam quality, respectively. Conversion of the non-linear dynamics to an MLD system is done as described in Section 2 of [11]. The resulting MLD system has 7 states - $p[k]$, $p_0[k]$, $p_f[k]$, $X_w[k-1]$, $u_1[k-1]$, $u_2[k-1]$ and $u_3[k-1]$, 3 inputs, 64 continuous and 45 binary auxiliary variables and $n_c = 414$. The system is subject to the following constraints:

$$\begin{aligned} \left| \frac{u_1[k] - u_1[k-1]}{T_s} \right| &\leq 0.007, & \left| \frac{u_3[k] - u_3[k-1]}{T_s} \right| &\leq 0.05, \\ -2 \leq \frac{u_2[k] - u_2[k-1]}{T_s} &\leq 0.02, & \left| \frac{X_w[k] - X_w[k-1]}{T_s} \right| &\leq 0.02. \end{aligned}$$

2) *Stage cost function*: The stage cost depends only on the state with $Q = \text{diag}([742, 441, 1, \epsilon, \epsilon, \epsilon, \epsilon])$ where $\epsilon = 10^{-9}$ and R a 3×3 zero matrix. The operations in computing the cuts are modified to remove the dependency on R . x_g is the *normal* operating point $p = 108$, $p_0 = 66.65$, $p_f = 428$ along with the corresponding equilibrium inputs $u_1 = 0.34$, $u_2 = 0.684$, $u_3 = 0.435$ and $X_w = 0.0129$.

3) *$Q^{(N)}$ -function approximation*: Let us denote the operational ranges of p , p_0 and p_f using \mathcal{R}_p , \mathcal{R}_{p_0} and \mathcal{R}_{p_f} . The size of this system makes it computationally expensive to train $Q^{(N)}$ -functions for long horizon lengths. We run Alg. 1 using $N = 6$ over \mathcal{X}_{Alg} with 256 data points distributed uniformly in $\mathcal{R}_p \times \mathcal{R}_{p_0} \times \mathcal{R}_{p_f}$, using $I_{max} = 200$ and $\eta_{min} = 10^{-3}$. The trained approximation, $Q_{200, \tilde{\beta}}^{(6)}$, has $I = 200$. We build the approximations $Q_{I, \tilde{\beta}}^{(6)}$ using the first $I = 25, 50, 75, 100, 125$ and 150 cuts. To demonstrate the advantage of the improvement metric $\tilde{\beta}$ over β we train an approximation by running Alg. 1 using the improvement metric β instead of $\tilde{\beta}$. Setting $I_{max} = 150$ and $\eta_{min} = 10^{-3}$, we train the approximation $Q_{150, \beta}^{(6)}$ with $I = 150$ cuts. We build the approximations $Q_{I, \beta}^{(6)}$ using the first $I = 25, 50, 75, 100$ and 125 cuts.

4) *Simulations using $Q^{(N)}$* : We compare the closed-loop costs of HMPC, with the LQR terminal cost which just uses the 3×3 principal submatrix of Q , against those of applying (5) derived from $Q_{I, \tilde{\beta}}^{(6)}$ and $Q_{I, \beta}^{(6)}$, for various values of I from 100 initial conditions spread uniformly across $\mathcal{R}_p \times \mathcal{R}_{p_0} \times \mathcal{R}_{p_f}$ in Table II. The performance of our controllers is close to that of HMPC $N = 6$ with our controllers outperforming it at several points. The average time taken to compute the policy is $0.6s$ for HMPC $N = 6$, $0.88s$ for $\pi(x; Q_{100, \beta}^{(6)})$, $0.88s$ for $\pi(x; Q_{100, \tilde{\beta}}^{(6)})$, $1.01s$ for $\pi(x; Q_{150, \tilde{\beta}}^{(6)})$, $1.23s$ for $\pi(x; Q_{200, \tilde{\beta}}^{(6)})$ and $21.78s$ for HMPC $N = 20$. The controller derived from our approximations and HMPC $N = 6$ have closed-loop costs within 2.5% of HMPC $N = 20$ at a fraction of the computation cost.

For $I = 25, 50, 75$ and 100 the closed-loop performance of $\pi(x; Q_{I, \tilde{\beta}}^{(6)})$ was seen to be better than that of $\pi(x; Q_{I, \beta}^{(6)})$ but the performance was similar for $I = 125$ and 150 , so using approximations built with the metric $\tilde{\beta}$ is better for small I . For $N = 6$ and $I = 100$, solving the MIQCQP controller of [7] for this system would require in excess of $1.25s$, 42% higher than our controller. On computing $Q_{100, \tilde{\beta}}^{(6)}$ at 2592 points distributed uniformly across $\mathcal{R}_p \times \mathcal{R}_{p_0} \times \mathcal{R}_{p_f}$, it is seen that q_0 is not at all used, whereas, an approximation trained with the same parameters and metric using the formulation in [7] uses q_0 at 1812 of these points.

V. CONCLUSIONS

We presented a new formulation for the lower bounding functions that are used in the $Q^{(N)}$ -function approximations along with a modified algorithm that improves the performance of our controller. We show that our controller can achieve good control performance on real-world examples through simulations on the traction control problem and

TABLE II

COMPARISON OF CLOSED-LOOP COSTS AGAINST HMPC FOR THE BOILER-TURBINE SYSTEM ($Q_I^{(N)}$ IS AN APPROXIMATION OF HORIZON LENGTH N WITH I CUTS)

Baseline	π_1 : HMPC $N = 20$		π_1 : HMPC $N = 6$		
	% of points where π_1 is better than the baseline	Mean better performance (%) at points where π_1 is better	% of points where π_1 is better than the baseline	Mean better performance (%) at points where π_1 is better	Mean worse performance (%) at points where π_1 is worse
$\pi(x; Q_{25,\beta}^{(6)})$	100	2.93	96	0.92	0.01
$\pi(x; Q_{50,\beta}^{(6)})$	100	2.73	90	0.84	0.56
$\pi(x; Q_{75,\beta}^{(6)})$	100	2.41	84	0.56	0.54
$\pi(x; Q_{100,\beta}^{(6)})$	100	2.46	90	0.59	0.92
$\pi(x; Q_{125,\beta}^{(6)})$	100	2.24	81	0.38	0.44
$\pi(x; Q_{150,\beta}^{(6)})$	100	2.09	70	0.22	0.27
$\pi(x; Q_{25,\tilde{\beta}}^{(6)})$	100	2.65	86	0.73	0.09
$\pi(x; Q_{50,\tilde{\beta}}^{(6)})$	100	2.6	84	0.7	0.16
$\pi(x; Q_{75,\tilde{\beta}}^{(6)})$	100	2.33	73	0.44	0.08
$\pi(x; Q_{100,\tilde{\beta}}^{(6)})$	100	2.28	75	0.38	0.11
$\pi(x; Q_{125,\tilde{\beta}}^{(6)})$	100	2.31	76	0.4	0.06
$\pi(x; Q_{150,\tilde{\beta}}^{(6)})$	100	2.16	66	0.26	0.09
$\pi(x; Q_{200,\tilde{\beta}}^{(6)})$	100	2.07	57	0.22	0.16
HMPC $N = 6$	100	1.92	-	-	-

the boiler-turbine system. Our algorithm is shown to work well for systems with dimensions relevant for practical MPC problems with the performance of our controller comparable to that of HMPC with an equal horizon length. The closed-loop costs of our controller also come close to the costs of the optimal control policy (approximated by long horizon length HMPC).

VI. ACKNOWLEDGEMENTS

Research supported by the European Research Council (ERC) under the European Union’s Horizon 2020 research and innovation programme, grant agreement OCAL, No. 787845.

REFERENCES

- [1] M. Pasamontes, J. Álvarez, J. Guzmán, M. Berenguel, and E. Camacho, “Hybrid modeling of a solar-thermal heating facility,” *Solar Energy*, vol. 97, pp. 577–590, 2013.
- [2] J. Lack, M. J. Powell, and A. D. Ames, “Planar multi-contact bipedal walking using hybrid zero dynamics,” in *2014 IEEE International Conference on Robotics and Automation*, pp. 2582–2588, 2014.
- [3] F. Borrelli, A. Bemporad, M. Fodor, and D. Hrovat, “An MPC/hybrid system approach to traction control,” *IEEE Transactions on Control Systems Technology*, vol. 14, 2006.
- [4] A. Bemporad, F. Borrelli, and M. Morari, “Model predictive control based on linear programming - the explicit solution,” *IEEE Transactions on Automatic Control*, vol. 47, no. 12, pp. 1974–1985, 2002.
- [5] S. Chen, K. Saulnier, N. Atanasov, D. D. Lee, V. Kumar, G. J. Pappas, and M. Morari, “Approximating explicit model predictive control using constrained neural networks,” in *2018 Annual American Control Conference (ACC)*, pp. 1520–1527, 2018.
- [6] E. T. Maddalena, C. G. da S. Moraes, G. Waltrich, and C. N. Jones, “A neural network architecture to learn explicit MPC controllers from data,” 2019.
- [7] S. Menta, J. Warrington, J. Lygeros, and M. Morari, “Learning solutions to hybrid control problems using benders cuts,” in *2nd Learning for Dynamics and Control Conference, Berkley, USA*, 2020.
- [8] A. Bemporad and M. Morari, “Control of systems integrating logic, dynamics, and constraints,” *Automatica*, vol. 35, no. 3, pp. 407–427, 1999.
- [9] F. Borrelli, A. Bemporad, and M. Morari, *Predictive control for linear and hybrid systems*. Cambridge University Press, 2017.
- [10] J. Warrington, “Learning continuous Q-functions using generalized benders cuts,” in *Proceedings of the European Control Conference, Naples, Italy*, 2019.
- [11] M. Sarailoo, Z. Rahmani, and B. Rezaie, “Fuzzy predictive control of a boiler-turbine system based on a hybrid model system,” *Industrial & Engineering Chemistry Research*, vol. 53, no. 6, pp. 2362–2381, 2014.
- [12] S. Falkner, A. Klein, and F. Hutter, “BOHB: Robust and efficient hyperparameter optimization at scale,” in *Proceedings of the 35th International Conference on Machine Learning*, vol. 80, pp. 1437–1446, PMLR, 10–15 Jul 2018.

APPENDIX

The MLD constraint matrices corresponding to the traction control system (16) are given here:

$$\begin{aligned}
 E_1 = & \begin{bmatrix} 0 & 5.3781 \\ 0 & -5.3781 \\ 0 & 0 \\ 0 & 0 \\ 0 & 0 \\ 0 & 0 \\ -0.000424 & 6.17455 \\ 0.000424 & -6.17455 \\ 0 & 0 \\ 0 & 0 \\ 5.82575 \cdot 10^{-6} & -0.0848295 \\ -5.82575 \cdot 10^{-6} & 0.0848295 \\ 0 & 5.3781 \\ 0 & -5.3781 \\ -1 & 0 \\ 1 & 0 \\ -1 & 0 \\ 0 & 0 \\ 0 & -1 \\ 0 & 1 \\ 0 & 0 \\ 0 & 0 \\ 0 & 0 \\ 0 & 0 \\ 0 & 0 \\ 0 & 0 \\ 1 & 0 \end{bmatrix}, & E_2 = & \begin{bmatrix} 0 & -73.456664601 \\ 0 & 57.273443009 \\ 1 & 1 \\ -1 & -1 \\ -88.586529999 & 0 \\ -59.558523999 & 0 \\ 59.558523999 & 0 \\ 88.586529999 & 0 \\ -0.817065082 & 0 \\ -1.216723605 & 0 \\ 1.216723605 & 0 \\ 0.817065082 & 0 \\ 73.456664601 & 0 \\ -57.273443009 & 0 \\ 0 & 0 \\ 0 & 0 \\ 0 & 0 \\ 0 & 0 \\ 0 & 0 \\ 0 & 0 \\ 0 & 0 \\ 0 & 0 \\ 0 & 0 \\ 0 & 0 \end{bmatrix} \\
E_3 = & \begin{bmatrix} 0 & 0 \\ 0 & 0 \\ 0 & 0 \\ 0 & 0 \\ 1 & 0 \\ -1 & 0 \\ 1 & 0 \\ -1 & 0 \\ 0 & 1 \\ 0 & -1 \\ 0 & 1 \\ 0 & -1 \\ 0 & 0 \\ 0 & 0 \\ 0 & 0 \\ 0 & 0 \\ 0 & 0 \\ 0 & 0 \\ 0 & 0 \\ 0 & 0 \\ 0 & 0 \\ 0 & 0 \\ 0 & 0 \\ 0 & 0 \\ 0 & 0 \\ 0 & 0 \\ 0 & 0 \\ 0 & 0 \\ 0 & 0 \\ 0 & 0 \end{bmatrix}, & E_4 = & \begin{bmatrix} 0 & 0.152993521 & -0.713114094 \\ 0 & -0.152993521 & 0.713114094 \\ 0 & 0 & 0 \\ 0 & 0 & 0 \\ 0 & 0 & 0 \\ 0 & 0 & 0 \\ -0.000424 & -0.173399999 & 0.806695 \\ 0.000424 & 0.173399999 & -0.806695 \\ 0 & 0 & 0 \\ 0 & 0 & 0 \\ 5.82575 \cdot 10^{-6} & 0.002377759 & -0.011079999 \\ -5.82575 \cdot 10^{-6} & -0.002377759 & 0.011079999 \\ 0 & 0.152993521 & -0.713114094 \\ 0 & -0.152993521 & 0.713114094 \\ -1 & 0 & 0 \\ 1 & 0 & 0 \\ 0 & 0 & 0 \\ 0 & -0.719942405 & 3.355704698 \\ 0 & 0 & 0 \\ 0 & 0 & 0 \\ 0 & -10 & 0 \\ 0 & 10 & 0 \\ 0 & 0 & -1 \\ 0 & 0 & 1 \\ 0 & 0 & 0 \end{bmatrix}, & E_5 = & \begin{bmatrix} -0.61532 \\ 57.888762009 \\ 1 \\ -1 \\ 0 \\ 0 \\ 59.558523999 \\ 88.586529999 \\ 0 \\ 0 \\ 1.216723605 \\ 0.817065082 \\ 72.841344601 \\ 0.615319 \\ 176 \\ 20 \\ 40 \\ 0 \\ 0.193439319 \\ -0.193439319 \\ 2500 \\ 100 \\ 100 \\ 20 \\ 40 \end{bmatrix}
 \end{aligned}$$